Energy optimization of an electric vehicle charging station using a hybrid STA-GWO MPPT strategy

Samia Amrouni[1,2], Said Aissou[3], Rafik Medjoudj[1], Elyazid Amirouche[3], Nabil Benyahia[4], Abdelhakim Belkaid[5]
[1]Laboratoire LITAN École supérieure en Sciences et Technologies de l'Informatique et du Numérique RN 75, Bejaia, Algérie
[2]Department of Automation, Mouloud Mammeri University of Tizi-Ouzou, Tizi-Ouzou, Algeria
[3]Laboratoire de Maitrise des Energies Renouvelables (LMER), Faculté de Technologie, Université de Bejaia, Bejaia, Algérie
[4]ESME Research Lab, Ivry-sur-Seine, France
[5]Laboratoire de Technologie Industrielle et de l'Information (LTII), Faculté de Technologie, Université de Bejaia, Algérie

Article Info

Article history:

Received Jul 24, 2026
Revised Aug 17, 2026
Accepted Aug 24, 2026

Keywords:

Electric vehicles
EV charging stations
Grey wolf optimizer
MPPT
Photovoltaic systems
Super twisting algorithm

ABSTRACT

This paper presents a hybrid electric vehicle charging station powered by both a PV source and the utility grid, incorporating an energy management strategy that prioritizes the utilization of solar energy while exporting surplus power to the grid during periods of low charging demand. To enhance the performance of maximum power point tracking, a hybrid control strategy integrating the grey wolf optimizer (GWO) and the super-twisting algorithm (STA) is proposed. The GWO performs rapid global exploration to accurately identify the maximum power point, whereas the STA ensures precise, robust, and chattering-free tracking under steady-state operating conditions. The proposed system was modeled in MATLAB/Simulink and validated under a dynamic irradiance profile characterized by both abrupt and gradual variations. Simulation results demonstrate a convergence time of 2-3 ms, residual power oscillations below 0.1%, and an average tracking efficiency of 99.38%. Compared with conventional MPPT techniques, the proposed STA-GWO approach significantly suppresses steady-state oscillations, accelerates convergence, and prevents MPP tracking failure under rapid irradiance fluctuations through the global optimization capability of GWO. These findings highlight the effectiveness of the proposed hybrid MPPT strategy in improving the robustness, energy conversion efficiency, and grid integration capability of PV-powered EV charging stations, making it a promising solution for next-generation sustainable charging infrastructure.

This is an open access article under the CC BY-SA license.

Corresponding Author:

Said Aissou
Laboratoire de Maitrise des Energies Renouvelables (LMER), Faculté de Technologie
Université de Bejaia
Bejaia, Algérie
Email: said.aissou@univ-bejaia.dz

1. INTRODUCTION

The growth of electric vehicles (EVs), coupled with the expanding deployment of renewable energy sources, has become a key driver in reducing greenhouse gas emissions and dependence on fossil fuels [1], [2]. Photovoltaic (PV) energy plays a prominent role owing to abundant solar energy resources, the continuous decline in module costs, and its ease of integration into electrical infrastructure [3]. This trend is reflected in the remarkable growth of installed PV capacity, which rose from around 40 GW in 2010 to more than 2.26 TW by the end of 2024, before exceeding 2.9 TW in 2025 [4]. In this context, integrating PV systems into EV charging stations is a relevant solution for decarbonizing the transport sector while limiting reliance on the electrical grid. However, fully exploiting these infrastructures depends heavily on the ability of the PV generator to deliver maximum power despite climatic variations. Indeed, PV cells exhibit inherently nonlinear characteristics that are strongly dependent on solar irradiance and temperature: variations in irradiance mainly affect the generated current, while temperature fluctuations affect the output voltage, causing a continuous shift of the maximum power point (MPP) [5]. Consequently, maintaining optimal efficiency requires a permanent adjustment of the operating point in order to continuously extract the maximum available power [6]. In EV charging applications, where energy availability and conversion efficiency are critical, this function is generally performed by a DC/DC converter controlled by a maximum power point tracking (MPPT) algorithm. By dynamically adjusting the converter's duty cycle, the MPPT algorithm keeps the PV system near the MPP and thus improves overall efficiency [7]. Over the past few decades, a large number of MPPT techniques have been proposed. They can be grouped into three main families: conventional techniques, artificial-intelligence-based approaches, and bio-inspired optimization algorithms, each offering advantages but also limitations that restrict their performance under rapidly varying irradiance conditions [8]. Conventional techniques, notably perturb and observe (P&O) and incremental conductance (INC), remain widely used owing to their simplicity of implementation [6], [9]. However, their performance degrades under dynamic climatic conditions due to relatively slow convergence, persistent oscillations around the MPP, and high sensitivity to the choice of perturbation step, which can lead to significant energy losses.

Faced with these limitations, research has progressively turned toward intelligent approaches capable of improving MPP tracking in dynamic environments. Among these, fuzzy logic controllers (FLC) have attracted particular interest owing to their ability to handle the nonlinearities of the PV generator without a precise mathematical model [10]. By exploiting linguistic rules, these methods offer appreciable robustness against irradiance variations and system uncertainties. Their performance nevertheless remains highly dependent on the design of the membership functions and rule base, whose generally empirical tuning limits their generalization capability and motivates the use of optimization techniques to automate controller parameterization. Artificial neural networks (ANN) constitute another widely studied family [11]. Due to their ability to learn nonlinear behaviors, they quickly estimate the MPP from measured electrical quantities, with good adaptation to weather variations. Nevertheless, their performance depends directly on the quality and representativeness of the training data. Under operating conditions not encountered during training, their accuracy can decrease significantly. Moreover, their computational cost, training constraints, and limited interpretability still restrict their integration into certain embedded applications requiring real-time control.

To overcome these limitations, many studies have turned to bio-inspired optimization algorithms, such as genetic algorithms (GA) [11], particle swarm optimization (PSO) [12], grey wolf optimizer (GWO) [13], [14]. These methods stand out for their ability to efficiently search for the global power maximum, particularly under partial shading conditions where several MPPs appear, thereby reducing the risk of convergence toward a local optimum. This performance improvement, however, comes with increased algorithmic complexity, computation time, and number of parameters to be tuned, which can hinder their use in embedded systems subject to real-time constraints. More recently, robust control strategies, notably sliding mode control (SMC), have emerged as a promising alternative owing to their fast convergence and robustness against parametric uncertainties and external disturbances. However, their main drawback lies in the chattering phenomenon, which can cause control oscillations, increased switching losses, and degraded energy performance. To mitigate this limitation, higher-order sliding mode variants, in particular the super-twisting algorithm (STA), have been proposed to reduce oscillations while preserving controller robustness. Despite encouraging results, tuning the parameters of these approaches remains complex and highly dependent on operating conditions [15].

A critical analysis of these different families shows that no single MPPT strategy alone meets all the requirements of modern PV systems. This complementarity explains the growing interest in hybrid approaches, which aim to combine the advantages of several techniques to achieve an optimal trade-off between convergence speed, tracking accuracy, robustness, and feasibility of implementation on embedded platforms. In this perspective, combinations of artificial intelligence algorithms, bio-inspired methods, and robust control techniques, such as PSO–P&O, ANFIS–PSO, Fuzzy–GWO, or ANN–SMC, have demonstrated a notable improvement in convergence speed and tracking accuracy. Nevertheless, most of these strategies still face high algorithmic complexity, a large number of parameters to tune, sensitivity to initial conditions, and a computational load sometimes incompatible with real-time implementation on embedded systems [16]-[19]. Among these hybrid solutions, the combination of GWO and STA is of particular interest. The role of GWO is to determine the reference corresponding to the global MPP, while the STA ensures robust tracking of this reference by driving the power converter [20], [21]. This architecture makes it possible to separate the optimization and control functions, exploiting the global exploration capability of GWO and the dynamic performance of the STA. Such functional complementarity addresses the limitations identified in existing approaches and constitutes a promising solution for simultaneously improving MPPT accuracy, convergence speed, and operating stability under strongly variable environmental conditions.

Among the solutions likely to mitigate global warming is the integration of PV systems into EV charging infrastructure [2], [22]. In this paper, we present a study of an EV charging installation located in Béjaïa, Algeria, whose architecture is shown in Figure 1. The main contribution of this work lies in optimizing the power of the PV part. Under dynamic irradiance conditions, we propose to explore an MPPT algorithm built around two components: energy management and power optimization. The studied system includes two electrical energy sources, the grid and the PV generator. The interface between these two sources is managed by two relays (K_{pv} and K_{Grid}), and four scenarios are examined. Depending on the availability of the solar resource, the PV source is given priority, either to charge the EV battery or to inject energy into the grid; otherwise, the grid takes over to ensure charging. The proposed MPPT approach combines the STA with the GWO optimizer: the latter quickly locates the optimal operating point, while the STA acts as a precision regulator that maintains this point with accuracy and stability. The simulation results obtained under MATLAB/Simulink provide valuable insight into the effectiveness of the proposed MPPT control and highlight the strengths of this hybrid approach under various operating conditions.

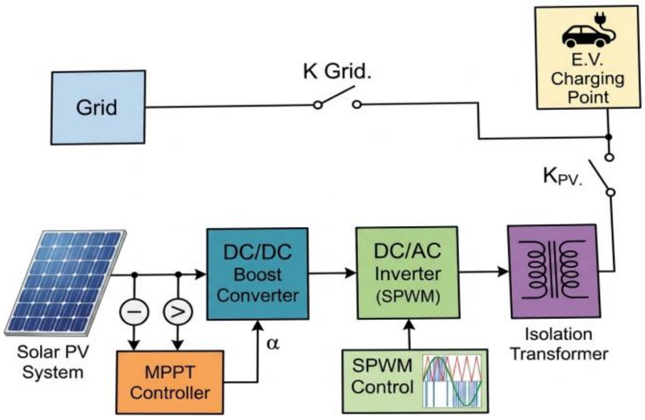

Figure 1. Schematic diagram of the proposed system

2. SYSTEM DESCRIPTION AND MODELLING

The proposed charging station is based on a hybrid architecture integrating a PV source and the single-phase electrical grid (220 V, 50 Hz). The overall system architecture is shown in Figure 2. This configuration aims to maximize the exploitation of solar energy while ensuring continuous power supply to the station by relying on the electrical grid when photovoltaic production becomes insufficient. The PV constitutes the main power source. To ensure optimal exploitation of this source, the PV chain is equipped with a boost-type DC/DC converter, controlled by an MPPT technique aimed at extracting, at every instant, the maximum power available from the photovoltaic generator.

The regulated direct current (DC) electrical energy at the output of the boost converter is then converted into alternating current (AC) energy by a DC/AC inverter controlled using the sinusoidal pulse width modulation (SPWM) technique [23]. This control method makes it possible to synthesize an AC voltage whose waveform is very close to a sine wave, thereby reducing the total harmonic distortion (THD) and improving the quality of the energy injected into the load or the grid. The inverter output is connected to an isolation transformer, which provides galvanic isolation between the photovoltaic chain and the electrical grid, voltage-level adaptation, and user safety.

The energy flow between the different sources is managed by means of two static switches, denoted (K_{PV}) and (K_{GRID}). The switch (K_{PV}) controls the connection of the photovoltaic chain to the charging station. When closed, the energy produced by the PV panels is preferentially directed toward charging the electric vehicle when a vehicle is connected to the station. Conversely, if no vehicle is present and PV production is in excess, this energy can be injected into the electrical grid, provided that the switch is closed (K_{GRID}).

When photovoltaic production becomes insufficient, particularly during periods of low sunlight, heavily overcast days, or at night, power supply priority is automatically transferred to the electrical grid. In this operating mode, K_{PV} is open while K_{GRID} is closed, allowing the grid to supply the energy needed to ensure continuity of the EV charging service. This strategy guarantees permanent availability of the station, regardless of fluctuations in solar production.

Thus, the proposed architecture ensures efficient power flow management by systematically prioritizing the use of PV energy, while using the electrical grid as a backup source when necessary. This approach improves self-consumption of the energy produced, reduces dependence on the grid, lowers the operating costs of the charging station, and contributes to reducing greenhouse gas emissions. The different operating priorities of switches K_{PV} and K_{GRID}, corresponding to the various management modes, are summarized in Table 1.

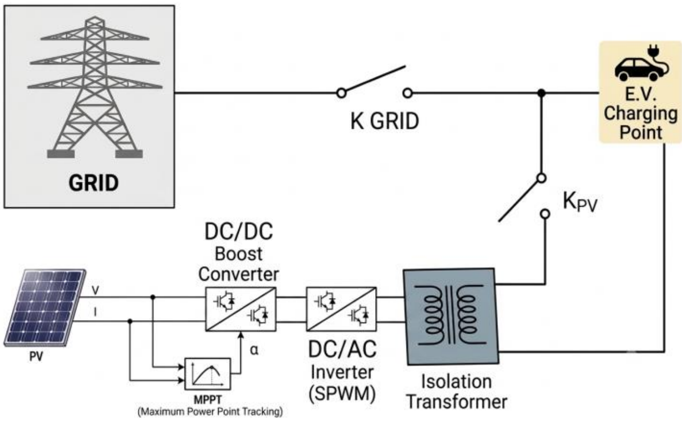

Figure 2. Architecture of the studied system

Table 1. Relay switching logic

K_{pv}	K_{Grid}	Results
0	0	0
1	0	PV to EV
0	1	Grid to EV
1	1	PV to Grid

2.1. PV modeling

The single-diode equivalent model, shown in Figure 3, is one of the most commonly used approaches for modeling photovoltaic cells. This wide adoption is explained by its relatively simple structure, while still offering sufficient accuracy to faithfully represent the electrical behavior of PV cells. By applying Kirchhoff's current law to the equivalent circuit presented, the expression of the various currents flowing in the photovoltaic cell is written as shown in (1) [24].

$$I_{PV} = I_{ph} - I_d - I_{Rsh} \tag{1}$$

Where I_{ph} represents the photocurrent generated by the photovoltaic cell, I_d denotes the current flowing through the diode, and I_{Rsh} corresponds to the current flowing through the shunt resistance (shunt). By substituting the currents I_d and I_{Rsh} with their respective expressions in (1), the expression of the output current of the photovoltaic cell is obtained, given by (2).

$$I_{PV} = I_{ph} - I_0 \cdot \left[exp\left(\frac{q\cdot(V_{PV}+R_S\cdot I_{PV})}{A\cdot N_S\cdot K\cdot T_j}\right) - 1\right] - \frac{V_{PV}+R_S\cdot I_{PV}}{R_{sh}} \tag{2}$$

The characteristic parameters of the photovoltaic panel are summarized in Table 2.

The (1) and (2) constitute the mathematical model of the photovoltaic panel, making it possible to reproduce its electrical behavior in the Simulink simulation environment. To evaluate the model's performance, several simulations were carried out under different solar irradiance levels. Figure 4 shows the characteristics obtained for irradiance values ranging from 200 to 1000 W/m², in steps of 200 W/m². The MPP are marked with red asterisks (*****). Table 2presents the photovoltaic panel parameters.

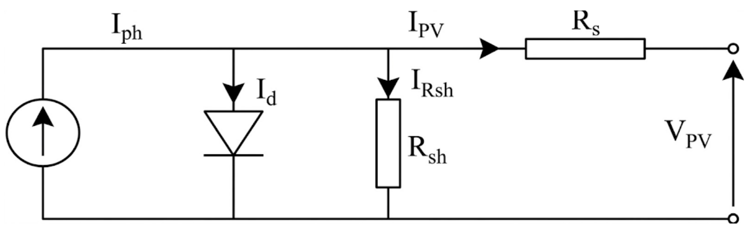

Figure 3. Equivalent circuit of solar cell

Table 2. Photovoltaic panel parameters

Symbol	Parameters	Values
P_{pv}	Photovoltaic power	80 Wp
I_{mppt}	Maximum current at MPP	4.65 A
V_{mppt}	Maximum voltage at MPP	17.5 V
I_{sc}	Short circuit current	4.95 A
V_{oc}	Open circuit voltage	21.9 V
α_{sc}	Temperature coefficient at short-current	3 mA/°C
β_{oc}	Voltage temperature coefficient of short-current	150 mV/°C

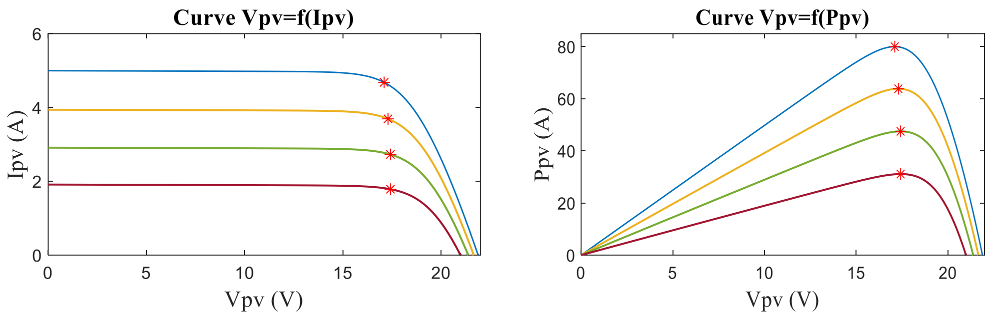

Figure 4. Photovoltaic STP80 IV and PV curves

2.2. DC-DC converter

DC–DC converters make it possible to regulate DC quantities by acting on the duty cycle of the semiconductor switch. In photovoltaic systems, they act as an adaptation interface between the PV generator and the load, adjusting voltage and current to ensure operation at the MPP while avoiding short-circuit conditions. Figure 5 shows the structure of a Boost converter, commonly used in photovoltaic installations. When the power switch (IGBT or MOSFET) is conducting, the energy supplied by the photovoltaic generator is stored in the inductor, while the diode is blocked. When the switch opens, the energy accumulated in the inductor adds to that delivered by the source to supply the load. The relationships linking the input and output voltages and currents of the converter are given by (3) [23].

$$V_{out} = \frac{V_{in}}{(1-\mathrm{D})} \qquad I_{in} = \frac{I_{out}}{(1-D)} \tag{3}$$

The dynamic equations of this converter are (4)-(6).

$$\begin{pmatrix} \frac{dI_L}{dt} = \frac{V_{pv}-V_0}{L} + \frac{V_0}{L}u \\ \frac{dV_0}{dt} = \left(-\frac{V_0}{RC} + \frac{I_L}{C}\right)\frac{V_0}{C}u \end{pmatrix} \tag{4}$$

$$\dot{X} = f(X) + b(X)u \tag{5}$$

$$f(X) = \begin{bmatrix} \frac{V_{pv}-V_0}{L} \\ \frac{-V_0}{RC} + \frac{I_L}{C} \end{bmatrix} \quad and \quad b(X) = \begin{bmatrix} \frac{V_0}{L} \\ \frac{-V_0}{C} \end{bmatrix} \tag{6}$$

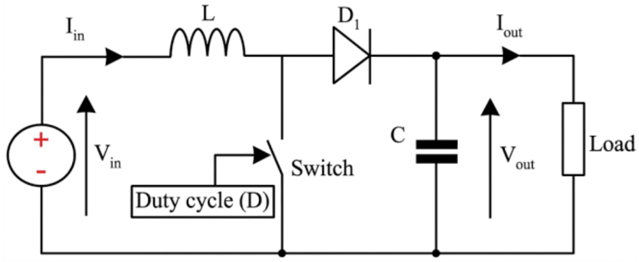

Figure 5. DC-DC boost converter power circuit

2.3. Maximum power point tracker algorithm

2.3.1. STA for MPPT

The STA is a robust control technique belonging to the family of higher-order sliding mode controllers. It was developed to retain the main advantages of classical sliding mode control, namely its robustness and tracking accuracy, while reducing the phenomenon known as chattering. In PV systems, the STA is used to adjust the duty cycle of the DC–DC converter in order to keep the generator near the MPP, even under rapid variations in irradiance and temperature. Its implementation relies on two essential steps: defining a sliding surface that guarantees rapid convergence toward the MPP, and then designing the STA control law that keeps the system states on this surface. Owing to its fast convergence and robustness against disturbances, the STA is a solution particularly well suited to advanced MPPT strategies [15], [25]. In this study, the sliding surface chosen for the STA control is defined from the MPPT optimality criterion. At the maximum power point, the derivative of the photovoltaic power with respect to voltage is zero. This criterion is then used to define a sliding surface guaranteeing the system's convergence toward the MPP. The sliding conditions are given by (7).

$$s^{\cdot}(x,t) = 0 \quad s(x,t) = \frac{\partial P_{pv}}{\partial V_{pv}} = V_{pv}\left(\frac{\partial I_{pv}}{\partial V_{pv}} + \frac{I_{pv}}{V_{pv}}\right) = 0 \tag{7}$$

Once the sliding surface has been defined, the next step consists of designing the control law that drives the system toward this surface and keeps it there despite model uncertainties and external disturbances. In this study, the duty cycle u of the boost converter is the control variable. To this end, super-twisting control is adopted. It relies on two complementary components: an equivalent control, which keeps the system on the sliding surface, and a discontinuous control, which guarantees fast convergence toward this surface as well as effective disturbance rejection. This combination improves the system's robustness and ensures accurate tracking of the maximum power point. The STA control law is then written as (8).

$$\begin{cases} u = u_{ec} + u_{sc} \\ u_{sc} = u_1 + u_2 \\ u_{ec} = -\frac{\left[\frac{ds}{dx}\right]^T f(x)}{\left[\frac{ds}{dx}\right]^T b(x)} = 1 - \frac{V_{PV}}{V_0} \end{cases} \tag{8}$$

Where u_{ec} represents the equivalent control ensuring the trajectory is maintained on the sliding surface, while u_{sc} corresponds to the super-twisting term ensuring finite-time convergence of the trajectory toward this surface while reducing the chattering phenomenon.

The equations for u_1 and u_2 are given by (9) and (10).

$$\begin{cases} u_1 = -\lambda |s|^{\frac{1}{2}} sign(s) \\ \frac{du_2}{dt} = -\gamma sign(s) \end{cases} \tag{9}$$

$$\gamma \text{ and } \lambda \text{ are gains such that} : \ \gamma > \frac{\Phi}{\Gamma_m} \ and \ \lambda > \sqrt{\frac{2}{\Gamma_m^2} \cdot \frac{(\Gamma_m \gamma + \Phi)^2}{\Gamma_m \gamma - \Phi}} \tag{10}$$

The finite-time convergence of the sliding surface to zero is established through a Lyapunov stability analysis. To this end, a positive definite candidate function is introduced in the form:

$$V(t) = \frac{1}{2}s^2(t) \tag{11}$$

In sliding mode control, the dynamics of the sliding surface are determined by its dependence on the state variables, expressed by (12).

$$S^{\cdot} = \left[\frac{\partial S}{\partial X}\right]^T X^{\cdot} = \left[\frac{\partial S}{\partial Ipv}\right]\left(-\frac{Vo}{L}(1-u) + \frac{Vpv}{L}\right) \tag{12}$$

The first term will be developed as (13).

$$\left[\frac{\partial S}{\partial Ipv}\right] = \frac{1}{V_{pv}} + \frac{q}{N_S n V_T}\frac{\partial Ipv}{\partial Vpv}\,\frac{\partial Vpv}{\partial Ipv} - \frac{\partial Vpv}{\partial Ipv}\,\frac{I_{pv}}{{V_{pv}}^2} \tag{13}$$

Such that:

$$\frac{\partial I_{pv}}{\partial V_{pv}} = -\left(\exp\left(\frac{q}{N_s \eta V_t}\right)\right)\cdot\frac{q}{N_s \eta V_t}\cdot I_d < 0 \tag{14}$$

V_{PV} is defined as in (15).

$$V_{pv} = \frac{N_s \eta\, V_T}{q}\ln\left(\frac{I_{ph} + I_d - I_{pv}}{I_d}\right) \tag{15}$$

The derivative of (15) can be written as (16).

$$\frac{\partial V_{pv}}{\partial I_{pv}} = -\left(ln\left(\frac{I_d}{I_{ph} + I_d - I_{pv}}\right)\right)\frac{N_s \eta\, V_T}{q} < 0 \tag{16}$$

The second term is as (17) and (18).

$$\dot{X} = -\left(\frac{V_0}{L}\right)(1 - u) + \left(\frac{V_{pv}}{L}\right) = -\left(\frac{V_o}{L}\right)(1 - u_{ec} - u_{STA}) + \left(\frac{V_{PV}}{L}\right) \tag{17}$$

$$= \frac{V_o}{L}\left(-\lambda\,|S|^{\frac{1}{2}} sign(S) - \int \gamma\, sign(S)\right) \tag{18}$$

According to (18), we have (19).

$$S\dot{S} = S\left[\frac{\partial S}{\partial I_{pv}}\right]\frac{V_o}{L}\left(-\lambda\,|S|^{\frac{1}{2}} sign(S) - \int \gamma\, sign(S)\right) \tag{19}$$

Consequently, it can be concluded that Lyapunov stability is ensured, since S and its derivative $\dot{S}$ systematically have opposite signs. The STA gains and were selected based on the tuning procedure reported in [20]. Accordingly, $\lambda = 0.051631$ and $\gamma = 0.006629$ were adopted in the present study and kept fixed throughout the simulations.

2.3.2. GWO-based optimal duty-cycle search

The GWO is a bio-inspired metaheuristic technique based on the social behavior and hierarchical hunting strategy of grey wolves in a pack [13]. This approach distributes solution agents across four hierarchical levels: α, β, δ, and ω, corresponding respectively to the best solution, the second-best, the third-best, and the remaining set of solutions. The α agent guides the optimization process by directing the search toward the most promising solution, while the β and δ agents refine this trajectory. The ω agents explore less favorable regions of the search space, thereby helping to maintain population diversity and limit the risk of premature convergence toward a local optimum.

Inspired by this hunting behavior, the GWO optimization process relies on three successive phases: target location, encircling, and the final attack. In the context of MPPT, each GWO agent represents a candidate value of the boost converter's duty cycle. The agents cooperate to search for the duty cycle value that extracts the maximum power from the photovoltaic generator. As the iterations progress, the agents' positions are adjusted, gradually leading to convergence toward the optimal duty cycle corresponding to the maximum power point.

The encircling behavior characteristic of pack hunting is then translated mathematically into a system of equations, making it possible to model the adaptive positioning of the solution agents around the sought optimum, as detailed in (20)-(23).

$$\vec{D} = \left| \vec{C} \cdot \overrightarrow{X_p} - \vec{X}(t) \right| \tag{20}$$

$$\vec{X}(t+1) = \overrightarrow{X_p}(t) - \vec{D} \cdot \vec{A} \tag{21}$$

D: the distance between wolf ω and the prey; t: current iteration; $\overrightarrow{X_P}$: position of the prey; and $\vec{X}$: position of the wolf. The vectors $\vec{A}$ and $\vec{C}$ are defined as (22) and (23).

$$\vec{A} = 2\,\vec{a} \cdot \overrightarrow{r_1} - \vec{a} \tag{22}$$

$$\vec{C} = 2\,\overrightarrow{r_2} \tag{23}$$

A coefficient decreasing linearly from 2 to 0 over the iterations ensuring the progressive transition between exploration and exploitation. $\vec{r}_1$ and $\vec{r}_2$: $random\ vectors \in [0,1]$, introducing a random component that diversifies exploration and thus avoids trapping in a local optimum.

Since the exact position of the MPPT is not known a priori, the GWO relies on the three best candidate solutions α, β, and δ to provide an estimate. In the context of MPPT, these three leaders correspond to the duty cycle values associated with the highest photovoltaic power values. The remaining agents then update their position based on these three leaders, according to (24).

$$\overrightarrow{D_\alpha} = \left| \overrightarrow{C_1} \overrightarrow{X_\alpha} - \vec{X} \right|, \overrightarrow{D_\beta} = \left| \overrightarrow{C_2} \overrightarrow{X_\beta} - \vec{X} \right|, \overrightarrow{D_\delta} = \left| \overrightarrow{C_3} \overrightarrow{X_\delta} - \vec{X} \right| \tag{24}$$

Each candidate duty cycle value is updated based on the three leaders α, β, and δ, which jointly guide the search toward the duty cycle corresponding to the MPPT, according to the following system of equations:

$$\begin{cases} \overrightarrow{X_1} = \overrightarrow{X_\alpha} - \overrightarrow{A_1}\left(\overrightarrow{D_\alpha}\right) \\ \overrightarrow{X_2} = \overrightarrow{X_\beta} - \overrightarrow{A_2}\left(\overrightarrow{D_\beta}\right) \\ \overrightarrow{X_3} = \overrightarrow{X_\delta} - \overrightarrow{A_3}\left(\overrightarrow{D_\delta}\right) \end{cases} \tag{25}$$

At each iteration, the position of each candidate solution is updated from the weighted average of the three positions estimated by the leaders α, β, and δ.

$$\vec{X}(t+1) = \frac{1}{3}\left(\overrightarrow{X_1} + \overrightarrow{X_2} + \overrightarrow{X_3}\right) \tag{26}$$

The GWO procedure for finding the maximum power point is summarized in Figure 6, which illustrates the main steps of computing and updating the duty cycle.

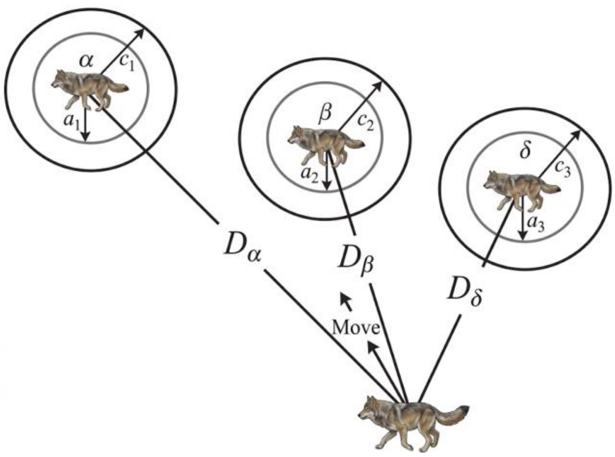

Figure 6. Encircling mechanism of the GWO algorithm based on the positions of leaders α, β, and δ [13]

3. RESULTS AND DISCUSSION

To evaluate the performance of the hybrid STA-GWO strategy in tracking the maximum power point, the photovoltaic system is subjected to a variable irradiance profile, shown in Figure 7. This profile was designed to reproduce atmospheric conditions representative of real operation, combining constant irradiance steps, abrupt transitions, and progressive ramps, so as to jointly stress the steady-state and dynamic regimes of the system. The constant irradiance steps (1000, 850, 800, 700, 600, 500, and 400 W/m²) are used to characterize the behavior of the STA controller in steady state. The analysis relies on two quantitative indicators, namely the stability of the extracted power around the maximum power point and the amplitude of the residual oscillations, which respectively reflect the tracking accuracy and the robustness of the control in steady-state operation. The abrupt irradiance variations observed at t = 1.2 s, 2.5 s, 4.6 s, 7 s, 12.9 s, 16 s, and 18.5 s constitute perturbation tests designed to evaluate the dynamic robustness of the GWO algorithm. Each of these steps instantaneously shifts the position of the MPP, requiring the controller to rapidly relocate the global optimum. The performance analysis relies on four quantitative indicators: the convergence time, reflecting the speed of relocation; the transient power loss, corresponding to the energy not extracted during the search phase; the possible overshoot, indicative of oscillatory behavior around the new equilibrium point; and the localization accuracy, measured by the residual deviation between the stabilized power and the theoretical maximum power available at the new irradiance. In addition, two increasing irradiance ramps are introduced, between 2.5 s and 4.6 s (from 400 to 700 W/m²) and between 9 s and 12.9 s (from 600 to 1000 W/m²), respectively. These progressive variations are intended to evaluate the performance of the hybrid STA-GWO strategy in a context where the maximum power point evolves continuously rather than through discrete jumps. They thus make it possible to verify the ability of the STA control to ensure continuous MPP tracking, while the GWO algorithm continuously adapts its search for the new optimal position, illustrating the functional synergy between the two components of the proposed approach. In this study, the GWO algorithm is configured with a population of 15 wolves (search agents) and a maximum of 40 iterations. This configuration represents a trade-off between convergence speed, accuracy in locating the maximum power point, and computational load, the latter having to remain compatible with the constraints of a real-time implementation. This test scenario thus makes it possible to jointly characterize the static performance of the STA control, related to MPP maintenance in steady state, and the dynamic performance of the GWO algorithm, related to the search for and rapid localization of the new MPP following a perturbation or during a continuous irradiance variation. This functional synergy highlights the value of the hybrid STA-GWO approach, which contributes to improving the robustness, convergence speed, and overall efficiency of the photovoltaic system under variable irradiance conditions.

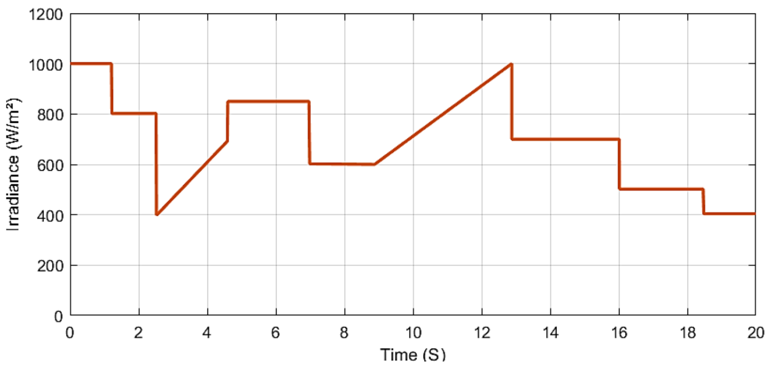

Figure 7. Dynamic irradiance profile

The dynamic response of the PV system is illustrated in Figures 8-10, representing the current, voltage, and output power, respectively, under the dynamic irradiance profile. The obtained waveforms reveal rapid stabilization around the maximum power point, accompanied by stable and robust tracking throughout the imposed irradiance variations. These results highlight the performance of the hybrid STA-GWO MPPT strategy, characterized by fast convergence, negligible oscillations in steady state, and high energy conversion efficiency over the entire irradiance range studied.

This tracking accuracy is of direct relevance to the operation of the studied electric vehicle charging station: by minimizing transient losses and maximizing the effectively extracted photovoltaic power, the STA-GWO strategy increases the share of solar energy directly available for charging the vehicle ("PV to EV" mode), thereby reducing reliance on grid energy ("Grid to EV" mode) according to the switching logic presented in Table 1. This efficiency gain, although limited to a few watts per transition, translates on a daily scale into a significant improvement in the photovoltaic self-consumption rate and a corresponding reduction in the station's operating costs.

The zoomed views in Figure 10 highlight the transient behavior of the PV power during successive irradiance changes. Each transition causes a brief decrease in power, resulting from the MPP shift, whose relocation by the STA-GWO algorithm requires only a very short time. This drop nevertheless remains limited to a few watts across all cases studied, before the power progressively returns to the new optimal value corresponding to the new irradiance level.

This fast response results in a convergence time on the order of 2 to 3 ms, significantly reducing energy losses during transient phases and ensuring efficient operation of the photovoltaic system. Once steady state is reached, the power stabilizes with residual oscillations below 0.1% of the nominal value, illustrating the ability of the super-twisting controller to limit the chattering phenomenon typically observed with conventional sliding-mode controls.

This behavior is reproducible across all tested irradiance levels (800, 700, 600, 500, and 400 W/m²): regardless of the variation amplitude, the STA-GWO algorithm rapidly converges toward the new maximum power point, without significant overshoot and with excellent steady-state stability. These qualitative observations are confirmed by the quantitative results presented in Table 3, comparing the theoretical maximum power with the power extracted by the STA-GWO control for each irradiance level studied.

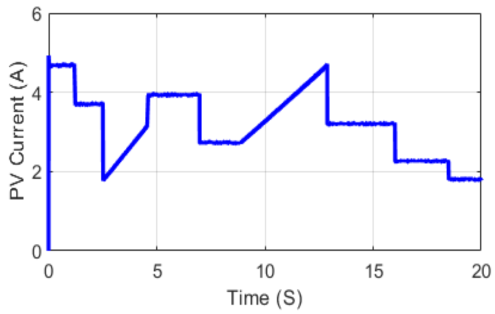

Figure 8. PV current response under dynamic irradiance

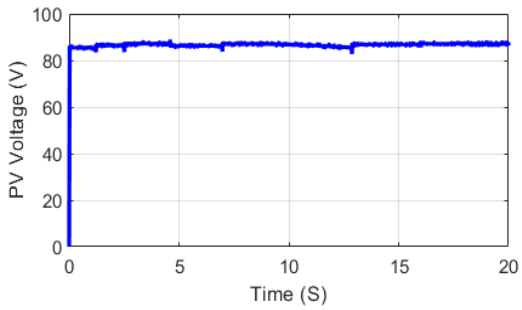

Figure 9. PV voltage response under dynamic irradiance

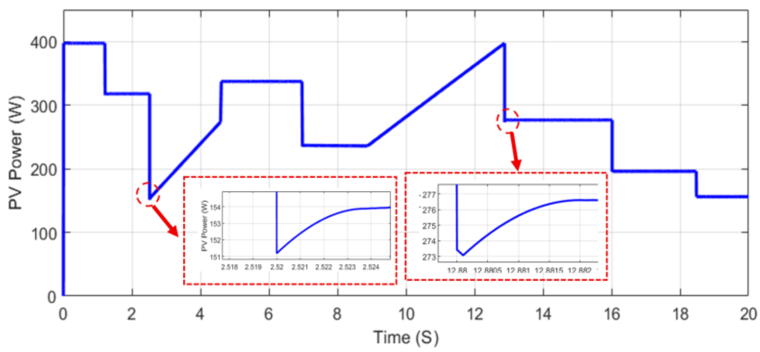

Figure 10. PV power response under dynamic irradiance

The corresponding calculations are defined as (27)-(29).

$$Deviation\ (\mathrm{W}) = (P_{\max} - P_{\mathrm{GWO}}) \tag{27}$$

$$\mathrm{Error}\ (\%) = \left(\frac{|P_{\max} - P_{\mathrm{GWO}}|}{P_{\max}} \times 100\right) \tag{28}$$

$$\text{Efficiency (\%)} = \left(\frac{P_{\text{GWO}}}{P_{\max}} \times 100 = 100 - \text{Error}\right) \quad (29)$$

The first indicator (deviation) expresses, in absolute terms, the amount of power not extracted relative to the theoretical maximum available; the second (error) normalizes this deviation as a percentage, allowing a consistent comparison across the different irradiance levels; the third (efficiency) directly reflects the proportion of power effectively captured by the STA-GWO control, and constitutes the most representative overall performance indicator. The results show that the hybrid STA-GWO ensures very accurate tracking of the MPP across all irradiance levels studied. The tracking efficiency ranges between 99.30% and 99.61%, with an average efficiency of approximately 99.38%.

The deviation between the theoretical maximum power $((P_{\max}))$and the power extracted by the STA-GWO control remains below 2.64 W, while the associated relative error does not exceed 0.70%. These values demonstrate the ability of the STA-GWO strategy to converge efficiently toward the MPP, regardless of the imposed irradiance conditions. The consistency of the efficiencies obtained across the entire irradiance range further confirms the robustness of the approach, demonstrating its suitability for use in photovoltaic systems subject to frequent variations in solar irradiance. To place the proposed approach in the context of existing MPPT techniques, Table 4 summarizes the main strengths and limitations of representative methods reported in the literature and compares them qualitatively with the proposed STA–GWO strategy.

Table 3. Comparison between theoretical maximum power and power extracted by the STA-GWO control, for different irradiance levels

E (W/m²)	Pmax (W)	P STA-GWO (W)	Deviation (W)	Error (%)	Efficiency (%)
1000	400.00	397.40	2.60	0.65	99.35
850	339.48	337.30	2.18	0.64	99.36
800	319.17	317.93	1.24	0.39	99.61
700	278.46	276.51	1.95	0.70	99.30
600	237.45	235.95	1.50	0.63	99.37
500	197.23	195.88	1.35	0.68	99.32
400	157.15	156.10	1.05	0.67	99.33

Table 4. Comparative analysis of representative MPPT methods and the proposed STA–GWO approach

Method	Main strengths	Main limitations
P&O	Simple implementation and low computational cost.	Slow convergence ≈ 0.32 s, steady-state oscillations, reduced performance under rapidly changing irradiance efficiency 97.9% [6]
INC	Higher tracking accuracy 98.6% than P&O and improved dynamic response.	Convergence ≈ 0.18 s, Sensitive to measurement noise and rapid environmental variations [6], [9]
PSO	Effective global optimization capability and good GMPP search	High computational burden and possible premature convergence [12], [16]
GWO	Fast convergence, efficient GMPP tracking, and good performance under partial shading conditions	Performance depends on parameter tuning and search-agent configuration [14]
STA	High robustness, finite-time convergence, and reduced chattering	Controller gain tuning remains challenging and requires stability analysis [15], [20], [25]
Proposed STA-GWO	Combines the global search capability of GWO with the robustness of STA, providing accurate and stable MPPT	Increased implementation complexity due to the hybrid optimization–control architecture

4. CONCLUSION

This paper presented STA–GWO MPPT strategy for a PV-assisted EV charging station operating under dynamic irradiance conditions. The proposed approach combines the global optimization capability of the GWO with the robustness of the STA, aiming to achieve fast, accurate, and stable maximum power point tracking under both uniform and rapidly varying solar irradiance. Simulation results demonstrated the effectiveness of the proposed strategy. The STA–GWO controller achieved a convergence time of 2–3 ms following irradiance variations, maintained steady-state oscillations below 0.1%, and reached an average MPPT tracking efficiency of 99.38% over all tested irradiance scenarios. Moreover, the deviation between the extracted power and the theoretical maximum power remained below 2.64 W, confirming the high tracking accuracy and robustness of the proposed approach under dynamic operating conditions.

A qualitative comparison with representative MPPT methods further highlights that the proposed STA–GWO strategy effectively combines the rapid global search capability of GWO with the robust tracking performance of STA. Consequently, the proposed hybrid approach offers improved dynamic response, enhanced tracking stability, and efficient energy extraction, making it a promising solution for photovoltaic-based electric vehicle charging applications. Future work will focus on extending the proposed strategy through the integration of a realistic electric vehicle battery charging model and BMS, while also considering practical uncertainties such as measurement noise, parameter variations, temperature changes, converter non-idealities, and load disturbances, followed by experimental validation using a real-time hardware platform to further assess its practical applicability.

FUNDING INFORMATION

Authors state no funding involved.

AUTHOR CONTRIBUTIONS STATEMENT

This journal uses the Contributor Roles Taxonomy (CRediT) to recognize individual author contributions, reduce authorship disputes, and facilitate collaboration.

Name of Author	C	M	So	Va	Fo	I	R	D	O	E	Vi	Su	P	Fu
Samia Amrouni	✓	✓	✓	✓	✓	✓	✓	✓	✓	✓			✓	
Said Aissou	✓	✓	✓	✓		✓	✓			✓	✓	✓		
Rafik Medjoudj	✓	✓	✓		✓	✓	✓	✓		✓	✓		✓	✓
Elyazid Amirouche		✓		✓	✓		✓		✓		✓	✓		
Nabil Benyahia	✓			✓			✓			✓	✓	✓		
Abdelhakim Belkaid	✓			✓			✓		✓		✓		✓	

C : **C**onceptualization
M : **M**ethodology
So : **So**ftware
Va : **Va**lidation
Fo : **Fo**rmal analysis
I : **I**nvestigation
R : **R**esources
D : **D**ata Curation
O : Writing - **O**riginal Draft
E : Writing - Review & **E**diting
Vi : **Vi**sualization
Su : **Su**pervision
P : **P**roject administration
Fu : **Fu**nding acquisition

CONFLICT OF INTEREST STATEMENT

Authors state no conflict of interest.

DATA AVAILABILITY

All data underpinning the findings of this study are available from the corresponding author, [SA], upon reasonable request.

REFERENCES

[1] P. Friedlingstein *et al.*, "Global carbon budget 2023," *Earth System Science Data*, vol. 15, no. 12, pp. 5301–5369, Dec. 2023, doi: 10.5194/essd-15-5301-2023.
[2] A. Ali, H. H. H. Mousa, M. F. Shaaban, M. A. Azzouz, and A. S. A. Awad, "A comprehensive review on charging topologies and power electronic converter solutions for electric vehicles," *Journal of Modern Power Systems and Clean Energy*, vol. 12, no. 3, pp. 675–694, 2024, doi: 10.35833/MPCE.2023.000107.
[3] C. P. Ohanu, S. A. Rufai, and U. C. Oluchi, "A comprehensive review of recent developments in smart grid through renewable energy resources integration," *Heliyon*, vol. 10, no. 3, p. e25705, Feb. 2024, doi: 10.1016/j.heliyon.2024.e25705.
[4] S. J. Yaqoob *et al.*, "Advanced maximum power point tracking in photovoltaic systems: a comprehensive review of classical, AI-based, and metaheuristic optimization techniques," *Engineering Reports*, vol. 7, no. 9, Sep. 2025, doi: 10.1002/eng2.70404.
[5] S. Luciani, G. Coccia, S. Tomassetti, M. Pierantozzi, and G. Di Nicola, "Correction procedures for temperature and irradiance of photovoltaic modules: determination of series resistance and temperature coefficients by means of an indoor solar flash test device," *Tecnica Italiana-Italian Journal of Engineering Science*, vol. 65, no. 2–4, pp. 264–270, Jul. 2021, doi: 10.18280/ti-ijes.652-419.
[6] A. Devarakonda, N. Karuppiah, T. Selvaraj, P. Balachandran, R. Shanmugasundaram, and T. Senjyu, "A comparative analysis of maximum power point techniques for solar photovoltaic systems," *Energies*, vol. 15, no. 22, p. 8776, Nov. 2022, doi: 10.3390/en15228776.
[7] M. M. A. Awan, M. Y. Javed, A. B. Asghar, and K. Ejsmont, "Performance optimization of a ten check MPPT algorithm for an off-grid solar photovoltaic system," *Energies*, vol. 15, no. 6, p. 2104, Mar. 2022, doi: 10.3390/en15062104.
[8] L. Bhukya, N. R. Kedika, and S. R. Salkuti, "Enhanced maximum power point techniques for solar photovoltaic system under uniform insolation and partial shading conditions: a review," *Algorithms*, vol. 15, no. 10, p. 365, Sep. 2022, doi: 10.3390/a15100365.
[9] S. Motahhir, A. Chalh, A. El Ghzizal, and A. Derouich, "Development of a low-cost PV system using an improved INC algorithm and a PV panel Proteus model," *Journal of Cleaner Production*, vol. 204, pp. 355–365, Dec. 2018, doi: 10.1016/j.jclepro.2018.08.246.
[10] F. Yahiaoui *et al.*, "An experimental testing of optimized fuzzy logic-based MPPT for a standalone PV system using genetic algorithms," *Mathematical Problems in Engineering*, vol. 2023, no. 1, Jan. 2023, doi: 10.1155/2023/4176997.

[11] K. S. Garud, S. Jayaraj, and M. Lee, "A review on modeling of solar photovoltaic systems using artificial neural networks, fuzzy logic, genetic algorithm and hybrid models," *International Journal of Energy Research*, vol. 45, no. 1, pp. 6–35, Jan. 2021, doi: 10.1002/er.5608.

[12] S. H. Sheikh Ahmadi, M. Karami, M. Gholami, and R. Mirzaei, "Improving MPPT performance in PV systems based on integrating the incremental conductance and particle swarm optimization methods," *Iranian Journal of Science and Technology, Transactions of Electrical Engineering*, vol. 46, no. 1, pp. 27–39, Mar. 2022, doi: 10.1007/s40998-021-00459-0.

[13] S. Djabali, R. Sangrody, S. Taheri, A.-M. Cretu, M. Mehrasa, and H. Vahedi, "Stability analysis of grey wolf optimization for MPPT of photovoltaic systems," in *2025 IEEE Industry Applications Society Annual Meeting (IAS)*, IEEE, Jun. 2025, pp. 1–5. doi: 10.1109/IAS62731.2025.11061668.

[14] I. S. Millah, P. C. Chang, D. F. Teshome, R. K. Subroto, K. L. Lian, and J.-F. Lin, "An enhanced grey wolf optimization algorithm for photovoltaic maximum power point tracking control under partial shading conditions," *IEEE Open Journal of the Industrial Electronics Society*, vol. 3, pp. 392–408, 2022, doi: 10.1109/OJIES.2022.3179284.

[15] S. Ghosh, A. K. Singh, and S. Niwas Singh, "Modified super twisting sliding mode control of grid synchronized smart PV inverter," in *2025 IEEE Industry Applications Society Annual Meeting (IAS)*, IEEE, Jun. 2025, pp. 1–7. doi: 10.1109/IAS62731.2025.11061488.

[16] X. Zhang, B. Zhao, H. Cui, G. Zhao, Y. Li, and Y. Huangfu, "A hybrid global maximum power point tracking control method based on particle swarm optimization (PSO) and perturbation and observation (P&O)," *Electric Power Systems Research*, vol. 248, p. 111967, Nov. 2025, doi: 10.1016/j.epsr.2025.111967.

[17] N. Priyadarshi, S. Padmanaban, J. B. Holm-Nielsen, F. Blaabjerg, and M. S. Bhaskar, "An experimental estimation of hybrid ANFIS–PSO-based MPPT for PV grid integration under fluctuating sun irradiance," *IEEE Systems Journal*, vol. 14, no. 1, pp. 1218–1229, Mar. 2020, doi: 10.1109/JSYST.2019.2949083.

[18] B. Laxman, A. Annamraju, and N. V. Srikanth, "A grey wolf optimized fuzzy logic based MPPT for shaded solar photovoltaic systems in microgrids," *International Journal of Hydrogen Energy*, vol. 46, no. 18, pp. 10653–10665, Mar. 2021, doi: 10.1016/j.ijhydene.2020.12.158.

[19] M. K. Senapati, K. Al Jaafari, K. Al Hosani, R. K. Behera, and U. R. Muduli, "Enhanced PV energy harvesting: an integrated approach using ANN and SMC," in *2023 IEEE 3rd International Conference on Smart Technologies for Power, Energy and Control (STPEC)*, IEEE, Dec. 2023, pp. 1–6. doi: 10.1109/STPEC59253.2023.10431323.

[20] N. Deghfel, A. E. Badoud, A. A. Al-Ahmadi, M. Bajaj, I. Zaitsev, and S. S. M. Ghoneim, "Improving maximum power point tracking efficiency in solar photovoltaic systems using super-twisting algorithm and grey wolf optimizer," *IET Renewable Power Generation*, vol. 18, no. 15, pp. 3329–3354, Nov. 2024, doi: 10.1049/rpg2.13138.

[21] S. Hadji, S. Aissou, and A. Belkaid, "Super-twisting MPPT enhanced via grey wolf optimization for dynamic PV operation," *International Journal of Power Electronics and Drive Systems (IJPEDS)*, vol. 17, no. 2, p. 1475, Jun. 2026, doi: 10.11591/ijpeds.v17.i2.pp1475-1485.

[22] Y. Hakam, H. Ahessab, M. Tabaa, B. ELHadadi, and A. Gaga, "Hybrid ANN–GWO MPPT with MPC-based inverter control for efficient EV charging under partial shading conditions," *Science Progress*, vol. 108, no. 2, Apr. 2025, doi: 10.1177/00368504251331835.

[23] A. M. Abdel-hamed, A. M. Nasser, H. Shatla, and A. Refky, "An improved SPWM control approach with aid of ant lion optimization for minimizing the THD in multilevel inverters," *Scientific Reports*, vol. 15, no. 1, p. 1990, Jan. 2025, doi: 10.1038/s41598-024-84678-5.

[24] T. N. Olayiwola, S.-H. Hyun, and S.-J. Choi, "Photovoltaic modeling: a comprehensive analysis of the I–V characteristic curve," *Sustainability*, vol. 16, no. 1, p. 432, Jan. 2024, doi: 10.3390/su16010432.

[25] R. Benadli, D. Frey, Y. Lembeye, M. Bjaoui, B. Khiari, and A. Sellami, "A direct backstepping super-twisting algorithm controller MPPT for a standalone photovoltaic storage system: design and real-time implementation," *Journal of Solar Energy Engineering*, vol. 145, no. 6, Dec. 2023, doi: 10.1115/1.4062096.

BIOGRAPHIES OF AUTHORS

Samia Amrouni from the Computer Science and Digital Technologies, affiliated with the Laboratory of Computer Science and Advanced Digital Technologies (LITAN), Bejaia, Algeria. She studied at the University of Tizi Ouzou, Algeria, where she received her Magister's degree in Electrical Engineering in 2015 from the same university. Her research interests include renewable energy integration and power electrical analysis. She can be contacted at email: amrouni@estin.dz.

Said Aissou is currently a teacher in the Science and Technology department and conducts research activities at the Laboratory of Renewable Energy Mastery (LMER). He studied at the University of Bejaia, Algeria, where he received his Master's degree in Electrical Engineering in 2012 and later got his Ph.D. in Electrical Engineering from the same university in 2016. His research interests include renewable energy integration, power system analysis, and electric vehicles. He can be contacted at email: said.aissou@univ-bejaia.dz.

Rafik Medjoudj is received the Master. degree in Electromechanical Engineering from the University of Bejaia, Algeria, in 2009, and the Ph.D. degree in Control and Energy Conversion from the same university in 2014. He is currently an Assistant Professor at the Higher School of Computer Science and Digital Technologies (ESTIN), Amizour, Bejaia, Algeria, and is affiliated with the LITAN Laboratory at ESTIN. His research interests include the reliability of electro-energetic systems, predictive maintenance, and the application of artificial intelligence methods to improve energy efficiency. He can be contacted at email: medjoudj@estin.dz.

Elyazid Amirouche is currently a teacher in the Department of Technology, University of Bejaia, Algeria, and a member of the LMER laboratory in the same university. He studied at the University of Bejaia, Algeria, where he received his Master degree in Electrical Engineering in 2018 and later got his Ph.D. in Electrical Engineering from the same university in 2022. His principal fields of interest are power electronics, electrical machines and drives, faults detection, diagnosis, and post fault operation of multiphase machines. He can be contacted at email: elyazid.amirouche@univ-bejaia.dz.

Nabil Benyahia defended his Ph.D. in 2014 at University of Béjaia (Algeria) in optimization of electrical propulsion system: application of fuel cells and supercapacitors electric vehicle. Experimental works of his thesis was carried out at the CRTT of Saint-Nazaire and the Fuel Cell Laboratory (FC-LAB) at University of Belfort-Montbéliard. He has participated in several innovative projects in particular: Design of the newly initiated Rail Innovative Centre (RIC) based on power hardware in loop (P-HIL) demonstrator to meet the future propulsion systems for the rail at the university of Derby (UK), Design of an inverter based SiC component for high-speed magnet machines drives at ENSEM in Nancy, and Develop an experimental platform based on power hardware in the loop of PEM fuel cell and propeller for naval applications at naval academy research institute (Lanveoc). Currently, he is an assistant professor at ESME school. He can be contacted at email: nabil.benyahia@esme.fr.

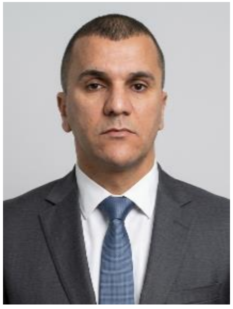

Abdelhakim Belkaid is received a B.Sc. degree and Magister degrees from the University of Bejaia, Algeria, in 1998 and 2004 respectively and a Doctorate degree in 2015 in Electrical Engineering from Setif University, Algeria. Currently, he is a professor and the deputy head of the ATE Department, Bejaia University, Algeria. His research interests include: wind and solar energy, power electronics, dc/dc converters, and renewable energy integration. He can be contacted at email: abdelhakim.belkaid@univ-bejaia.dz.